

Nomenclature

a_{imp}, b_{imp}	coefficients of spherical Bessel functions in radial eigenfunction (see Eq. (31))
A_{in}, B_{in}, C_{in}	coefficients in Eq. (4)
$A_{out}, B_{out}, C_{out}$	coefficients in Eq. (5)
$C_{1in}, C_{2in}, C_{1out}, C_{2out}$	coefficients in Eq. (35) dependent on inner and outer surface boundary conditions
D_{mp}	coefficient in general solution (Eq. (27)) dependent on initial condition
f_i	initial temperature distribution in the i th layer at $t = 0$
$f_p(r)$	particular integral in Eq. (42)
g_i	volumetric heat source distribution in the i th layer
h_{out}	outer surface heat transfer coefficient
$J_{m+0.5}$	Bessel function of the first kind of order $(m + 0.5)$
k_i	thermal conductivity of the i th layer
m	index
M	number of θ -direction eigenfunctions used in the solution
M_{rmp}	norms for r -direction
P	number of radial eigenfunction used in the solution corresponding to each θ -direction eigenvalue
$P_m(\mu)$	Legendre functions of the first kind of degree m
$Q_m(\mu)$	Legendre functions of the second kind of degree m
r	radial coordinate
r_i	outer radius of the i th layer

$R_{imp}(\lambda_{imp}r)$	radial eigenfunctions for the i th layer
S	volumetric heat source strength in layer-2 of illustrative problem
t	time
$T_i(r, \theta, t)$	temperature distribution in the i th layer
$Y_{m+0.5}$	Bessel function of the second kind of order $(m + 0.5)$
$x_{ij}, y_{ij}, j = 1, 2, 3, 4$	elements of $(2n \times 2n)$ matrix in Eq. (35)

Greek symbols

α_i	thermal diffusivity of the i th layer
$\Delta\lambda$	window size for evaluation of radial eigenvalues
θ	polar coordinate
μ	defined as $\mu = \cos \theta$ in Eq. (2)
ϕ	azimuth variable
β_m	θ -direction eigenvalues (degree of Legendre functions)
$\Theta_m(\mu)$	eigenfunctions in the polar direction
λ_{imp}	radial eigenvalues
ω_{1m}, ω_{2m}	coefficients in $\Theta_m(\mu)$ Eq. (28)

Subscripts and superscripts

i	layer or interface number
ss	steady-state
'	Differentiation

practical engineering problems. Time-dependent temperature distribution in a layered spherical fuel element in a pebble bed reactor with θ -dependent convective boundary condition may, for example, benefit from such solutions. Another relevant scenario that may also lead to θ -dependent temperature distribution is that of heat conduction in a *part*-spherical geometry i.e. $0 \leq \theta \leq \Psi$ and $\Psi < \pi$. Temperature in such a geometry is inherently dependent on θ due to the geometry itself and therefore, the temperature distribution is a function of at least two variables, r and θ .

This paper presents an analytical series solution for transient boundary-value problem of heat conduction in r - θ spherical coordinates. Proposed solution is applicable in spherical or *part*-spherical multilayer geometries in which temperature does not depend upon the ϕ variable, such as (see Fig. 1): spherical cone (a), hemisphere (b), spherical wedge (c), or full sphere (d). Spatially non-uniform (only r and θ -dependent), time-independent volumetric heat sources may be present in the layers. Inhomogeneous, time-independent, θ -dependent boundary conditions of the *first*, *second* or *third* kind may be applied on the inner and outer radial boundaries. However, only homogeneous boundary conditions of the *first* or *second* kind may be applied on the θ -direction boundary surfaces.

2. Mathematical formulation

Consider n concentric spherical shells in perfect thermal contact ($r_0 \leq r \leq r_n$, $0 \leq \theta \leq \Psi$ and $0 \leq \phi \leq 2\pi$), as shown schematically in Fig. 2. Different shapes shown in Fig. 1 can be obtained by varying the angle Ψ ($0 < \Psi \leq \pi$), such as a spherical cone ($\Psi < \pi/2$), a hemisphere ($\Psi = \pi/2$), a spherical wedge ($\Psi > \pi/2$) and a full sphere ($\Psi = \pi$). All the layers are assumed to be isotropic. Let k_i and α_i be the temperature independent thermal conductivity and thermal diffusivity of the i th layer. Initially, at $t = 0$, the i th layer is at a specified temperature $f_i(r, \theta)$. For $t > 0$, homogenous boundary conditions of either *first* or *second* kind can be applied on the inner ($i = 1, r = r_0$) and the outer ($i = n, r = r_n$) radial surfaces. In addition, spatially non-uniform, time-independent heat

sources $g_i(r, \theta)$ are switched on in each layer at $t = 0$. Here, none of the initial or boundary conditions or the heat generation rates depend on the azimuth (ϕ) variable. Hence, the temperature distribution is assumed to be azimuthally symmetric i.e. independent of ϕ .

Under these assumptions, governing heat conduction equation for the temperature in the i th layer $T_i(r, \theta, t)$, along with the boundary and initial conditions, can be written as follows:

Governing equation:

$$\frac{1}{\alpha_i} \frac{\partial T_i}{\partial t}(r, \theta, t) = \frac{1}{r^2} \frac{\partial}{\partial r} \left(r^2 \frac{\partial T_i}{\partial r}(r, \theta, t) \right) + \frac{1}{r^2 \sin \theta} \times \frac{\partial}{\partial \theta} \left(\sin \theta \frac{\partial T_i}{\partial \theta}(r, \theta, t) \right) + \frac{g_i(r, \theta)}{k_i},$$

$$r_{i-1} \leq r \leq r_i, \quad 1 \leq i \leq n \quad (1)$$

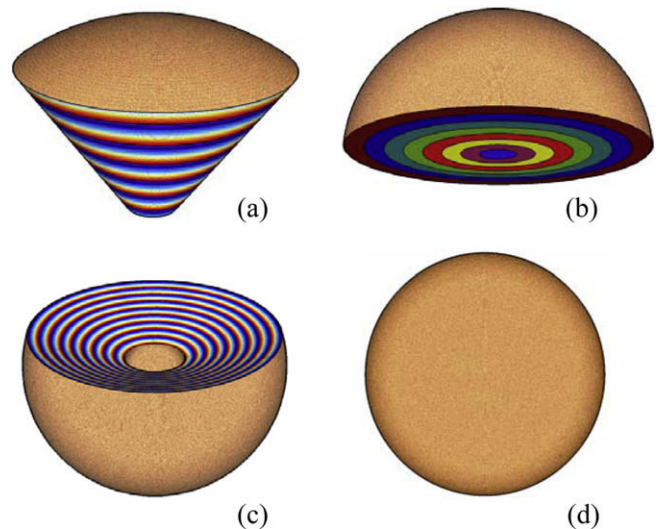


Fig. 1. 3D representation of azimuthally symmetric spherical and *part*-spherical multilayer geometries: (a) spherical cone; (b) hemisphere; (c) spherical wedge; and (d) full sphere.

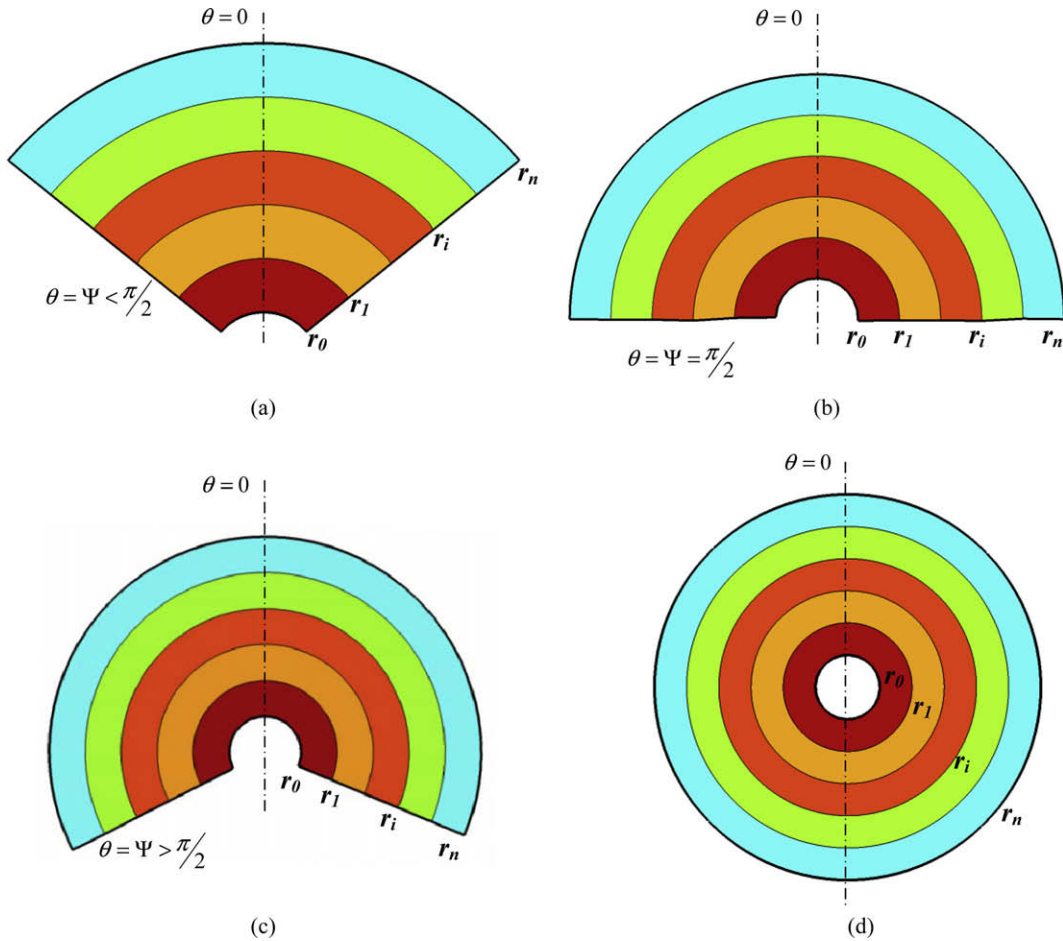


Fig. 2. 2D cross-sectional views of n concentric spherical layers ($r_0 \leq r \leq r_n$ and $0 \leq \theta \leq \Psi$). Layers are azimuthally symmetric ($0 \leq \phi \leq 2\pi$) and in perfect thermal contact. Different shapes can be characterized by varying the angle Ψ ($0 < \Psi \leq \pi$). (a) spherical cone, $\Psi < \pi/2$; (b) hemisphere, $\Psi = \pi/2$; (c) spherical wedge, $\Psi > \pi/2$ and (d) full sphere, $\Psi = \pi$.

Eq. (1) may be transformed in a more convenient form by defining a new independent variable μ as

$$\mu = \cos \theta \tag{2}$$

to yield

$$\frac{1}{\alpha_i} \frac{\partial T_i}{\partial t}(r, \mu, t) = \frac{1}{r^2} \frac{\partial}{\partial r} \left(r^2 \frac{\partial T_i}{\partial r}(r, \mu, t) \right) + \frac{1}{r^2} \times \frac{\partial}{\partial \mu} \left((1 - \mu^2) \frac{\partial T_i}{\partial \mu}(r, \mu, t) \right) + \frac{g_i(r, \mu)}{k_i},$$

$$r_{i-1} \leq r \leq r_i, \quad 1 \leq i \leq n \tag{3}$$

Boundary conditions:

- Inner surface of 1st layer ($i = 1$)

$$A_{in} \frac{\partial T_1}{\partial r}(r_0, \mu, t) + B_{in} T_1(r_0, \mu, t) = C_{in}(\mu) \tag{4}$$

- Outer surface of n th layer ($i = n$)

$$A_{out} \frac{\partial T_n}{\partial r}(r_n, \mu, t) + B_{out} T_n(r_n, \mu, t) = C_{out}(\mu) \tag{5}$$

- $\theta = \Psi$ surface ($i = 1, 2, \dots, n$)

$$T_i(r, \mu = \mu_\Psi, t) = 0 \text{ or } \frac{\partial T_i}{\partial \mu}(r, \mu = \mu_\Psi, t) = 0,$$

$$\mu_\Psi = \cos \Psi, \quad \Psi < \pi \tag{6}$$

- Interface of the i th layer ($i = 2, \dots, n$)

$$T_i(r_{i-1}, \mu, t) = T_{i-1}(r_{i-1}, \mu, t) \tag{7}$$

$$k_i \frac{\partial T_i}{\partial r}(r_{i-1}, \mu, t) = k_{i-1} \frac{\partial T_{i-1}}{\partial r}(r_{i-1}, \mu, t) \tag{8}$$

- Initial condition:

$$T_i(r, \mu, t = 0) = f_i(r, \mu) \tag{9}$$

It is to be noted that boundary conditions either of the *first*, *second* or *third* kind can be imposed on the inner ($r = r_0$) and outer ($r = r_n$) surfaces by choosing the coefficients in Eqs. (4) and (5) appropriately. Furthermore, heat conduction in a geometry with zero inner radius ($r_0 = 0$) can also be solved by assigning zero values to B_{in} and $C_{in}(\mu)$ in Eq. (4).

3. Solution methodology

To apply the *separation of variables method*, which is only applicable to homogenous transient problems, the non-homogenous problem described in Section 2 is split into a homogenous transient problem for $\bar{T}_i(r, \mu, t)$ and a non-homogenous steady state problem for $T_{ss,i}(r, \mu)$, where $\bar{T}_i(r, \mu, t) \equiv T_i(r, \mu, t) - T_{ss,i}(r, \mu)$. The governing equations for the two sub-problems are as follows:

4.3. θ -Direction eigencondition

Only homogenous boundary conditions of the *first* or *second* kind may be applied on $\theta = \Psi$ ($0 < \Psi < \pi$) surface. Boundary conditions, which are either inhomogeneous or are of the *third* kind, can not be employed in the θ -direction since they produces unconditional mathematical incompatibilities [13]. The θ -direction eigenfunctions $P_{\beta_m}(\mu)$ that satisfy these boundary conditions give the following eigencondition:

$$P_{\beta_m}(\mu = \mu_\psi) = 0 \text{ or } \frac{\partial P_{\beta_m}}{\partial \mu}(\mu = \mu_\psi) = 0, \quad -1 < \mu_\psi < 1. \quad (34)$$

Roots of Eq. (34) yield the eigenvalues β_m (indexed by an integer m).

For (multilayer) hemisphere and for full sphere, which are the most common spherical geometries, the θ -direction eigenvalues (β_m) can be determined without solving Eq. (34) by using some of the well known properties of the *Legendre functions*. In the case of a hemisphere ($\Psi = \pi/2$, ($0 \leq \mu \leq 1$)), a homogenous boundary condition of the *first kind* at the base (i.e. $P_{\beta_m}(\mu = 0) = 0$) is only satisfied when β_m are odd integers, i.e. $\beta_m = 1, 3, 5, \dots$. Similarly, a homogenous boundary condition of the *second kind* at the base (i.e. $\frac{dP_{\beta_m}}{d\mu}(\mu = 0) = 0$) is only satisfied for even integer values of β_m i.e. $\beta_m = 0, 2, 4, \dots$ [26]. In the case of a full sphere ($\Psi = \pi$, $-1 \leq \mu \leq 1$), eigenfunctions $P_{\beta_m}(\mu)$ at $\mu = -1$ are finite only for non-negative integer values of β_m , i.e., $\beta_m = 0, 1, 2, 3, \dots$. Fractional values of β_m are excluded from the solution due to the non-finiteness of eigenfunctions $P_{\beta_m}(\mu)$ at $\mu = -1$ [26].

4.4. Radial eigencondition

Application of the boundary conditions (11) and (12) and the interface conditions (14) and (15) to the radial eigenfunction $R_{imp}(\lambda_{imp}r)$ yields, for each m , the following $(2n \times 2n)$ matrix equation:

$$\begin{bmatrix} C_{1in} & C_{2in} & 0 & 0 & \dots & 0 & 0 & 0 & 0 & \dots & 0 & 0 & 0 & 0 & \dots & 0 & 0 & 0 & 0 \\ x_{11} & x_{12} & x_{13} & x_{14} & \dots & 0 & 0 & 0 & 0 & \dots & 0 & 0 & 0 & 0 & \dots & 0 & 0 & 0 & 0 \\ y_{11} & y_{12} & y_{13} & y_{14} & \dots & 0 & 0 & 0 & 0 & \dots & 0 & 0 & 0 & 0 & \dots & 0 & 0 & 0 & 0 \\ \dots & \dots & \dots & \dots & \dots & \dots & \dots & \dots & \dots & \dots & \dots & \dots & \dots & \dots & \dots & \dots & \dots & \dots & \dots \\ 0 & 0 & 0 & 0 & \dots & x_{i1} & x_{i2} & x_{i3} & x_{i4} & \dots & 0 & 0 & 0 & 0 & \dots & 0 & 0 & 0 & 0 \\ 0 & 0 & 0 & 0 & \dots & y_{i1} & y_{i2} & y_{i3} & y_{i4} & \dots & 0 & 0 & 0 & 0 & \dots & 0 & 0 & 0 & 0 \\ \dots & \dots & \dots & \dots & \dots & \dots & \dots & \dots & \dots & \dots & \dots & \dots & \dots & \dots & \dots & \dots & \dots & \dots & \dots \\ 0 & 0 & 0 & 0 & \dots & 0 & 0 & 0 & 0 & \dots & x_{n-1,1} & x_{n-1,2} & x_{n-1,3} & x_{n-1,4} & \dots & \dots & \dots & \dots \\ 0 & 0 & 0 & 0 & \dots & 0 & 0 & 0 & 0 & \dots & y_{n-1,1} & y_{n-1,2} & y_{n-1,3} & y_{n-1,4} & \dots & \dots & \dots & \dots \\ 0 & 0 & 0 & 0 & \dots & 0 & 0 & 0 & 0 & \dots & 0 & 0 & C_{1out} & C_{2out} & \dots & \dots & \dots & \dots & 0 \end{bmatrix} \begin{bmatrix} a_{1mp} \\ b_{1mp} \\ \dots \\ a_{imp} \\ b_{imp} \\ \dots \\ a_{nmp} \\ b_{nmp} \end{bmatrix} = \begin{bmatrix} 0 \\ 0 \\ \dots \\ 0 \\ 0 \\ \dots \\ 0 \\ 0 \end{bmatrix} \quad (35)$$

where

$$\begin{aligned} C_{1in} &= A_{in}R'_j(\lambda_{1mp}r_0) + B_{in}R_j(\lambda_{1mp}r_0) \\ C_{2in} &= A_{in}R'_Y(\lambda_{1mp}r_0) + B_{in}R_Y(\lambda_{1mp}r_0) \\ x_{i1} &= R_j(\lambda_{imp}r_i) \\ x_{i2} &= R_Y(\lambda_{imp}r_i) \\ x_{i3} &= -R_j(\lambda_{i+1,mp}r_i) \\ x_{i4} &= -R_Y(\lambda_{i+1,mp}r_i) \\ y_{i1} &= k_iR'_j(\lambda_{imp}r_i) \\ y_{i2} &= k_iR'_Y(\lambda_{imp}r_i) \\ y_{i3} &= -k_{i+1}R'_j(\lambda_{i+1,mp}r_i) \\ y_{i4} &= -k_{i+1}R'_Y(\lambda_{i+1,mp}r_i) \\ C_{1out} &= A_{out}R'_j(\lambda_{nmp}r_n) + B_{out}R_j(\lambda_{nmp}r_n) \\ C_{2out} &= A_{out}R'_Y(\lambda_{nmp}r_n) + B_{out}R_Y(\lambda_{nmp}r_n) \end{aligned}$$

and prime (') denotes differentiation.

In the above matrix equation, all λ_{imp} ($i \neq 1$) may be written in terms of λ_{1mp} using Eq. (33). Subsequently, radial eigencondition can be obtained by setting the determinant of the $(2n \times 2n)$ coefficient matrix in Eq. (35) equal to zero. Roots of which, in turn, yield the infinite number of eigenvalues λ_{1mp} corresponding to the first layer for each m .

In general, transverse eigenvalues for multilayer time-dependent heat conduction problems in Cartesian coordinates may be imaginary. Same is true for 2D (r, z) cylindrical coordinates [21]. These eigenvalues are imaginary due to the explicit dependence of the transverse eigenvalues on those in the remaining direction(s). However, in 2D r - θ spherical coordinate system, dependence of the radial eigenvalues on those in the other direction is not explicit. The same is also true for multilayer heat conduction problems in cylindrical polar coordinate system [21]. Consequently, absence of explicit dependence leads to a complete solution which does not have imaginary radial eigenvalues, and thus λ_{imp} are real [22–23].

4.5. Determination of coefficients a_{imp} and b_{imp}

Coefficients a_{imp} and b_{imp} in the radial eigenfunction $R_{imp}(\lambda_{imp}r)$ (Eq. (31)) are determined from the following recurrence relationship, obtained by imposing the i th interface condition (see Eqs. (14) and (15)), valid for $i \in [1, n - 1]$,

$$\begin{pmatrix} a_{i+1,mp} \\ b_{i+1,mp} \end{pmatrix} = \begin{pmatrix} R_j(\lambda_{i+1,mp}r_i) & R_Y(\lambda_{i+1,mp}r_i) \\ k_{i+1}R'_j(\lambda_{i+1,mp}r_i) & k_{i+1}R'_Y(\lambda_{i+1,mp}r_i) \end{pmatrix}^{-1} \begin{pmatrix} R_j(\lambda_{imp}r_i) & R_Y(\lambda_{imp}r_i) \\ k_iR'_j(\lambda_{imp}r_i) & k_iR'_Y(\lambda_{imp}r_i) \end{pmatrix} \begin{pmatrix} a_{imp} \\ b_{imp} \end{pmatrix} \quad (36)$$

where $b_{1mp} = -\frac{C_{1in}}{C_{2in}} a_{1mp}$ and a_{1mp} is arbitrary.

Clearly, two sets of eigenfunctions obtained with different a_{1mp} are proportional to each other and are equally valid solutions of the radial eigenvalue problem. Moreover, after the introduction of D_{mp} in the general solution (see Eq. (27)), there is no need to retain a_{1mp} or ω_{1m} as separate constants. [The above discussion is in fact true for any eigenvalue problem.]

4.6. Determination of coefficient D_{mp}

Coefficient D_{mp} in Eq. (27) may be obtained by applying the initial condition (16) and then making use of the orthogonality conditions, as follows:

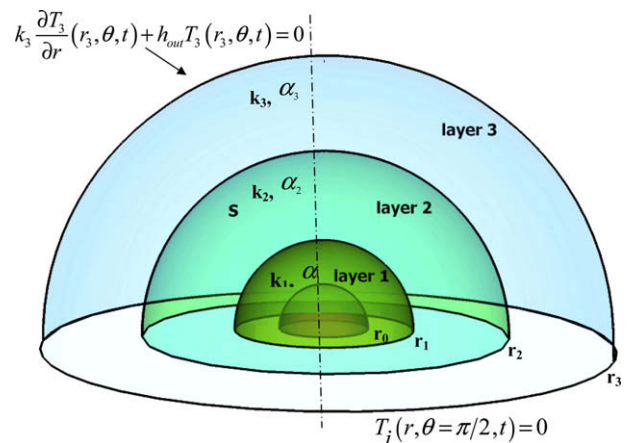


Fig. 3. Schematic diagram of the three-layer-hemisphere problem. Mixed boundary condition is applied at the outer radial surface of the hemisphere, while the base and the inner radial surface are kept at zero temperatures. Heat source of strength S is assumed to be uniformly distributed in layer-2.

$$D_{mp} = \frac{1}{M_{imp} N_m} \sum_{i=1}^n \frac{k_i}{\alpha_i} \int_{\mu_p}^1 \int_{r_{i-1}}^{r_i} r^2 R_{imp}(\lambda_{imp} r) P_{\beta_m}(\mu) \bar{T}_i(r, \mu, t = 0) dr d\mu \quad (37)$$

5. Solution to the inhomogeneous steady state problem

The inhomogeneous steady state problem is solved using eigenfunction expansion method. The steady state temperature distribution $T_{ss,i}(r, \mu)$, governed by Eq. (17), may be written as a generalized Fourier series in terms of θ -direction eigenfunctions $P_{\beta_m}(\mu)$,

$$T_{ss,i}(r, \mu) = \sum_{m=0}^{\infty} \hat{T}_{im}(r) P_{\beta_m}(\mu) \quad (38)$$

Substituting Eq. (38) in Eq. (17) leads to an ODE for $\hat{T}_{im}(r)$,

$$\frac{1}{r^2} \frac{d}{dr} \left(r^2 \frac{d\hat{T}_{im}(r)}{dr} \right) - \frac{\beta_m(\beta_m + 1)}{r^2} \hat{T}_{im}(r) + \frac{\hat{g}_{im}(r)}{k_i} = 0 \quad (39)$$

Note that the source term $g_i(r, \mu)$ is expanded in a generalized Fourier series as:

$$g_i(r, \mu) = \sum_{m=0}^{\infty} \hat{g}_{im}(r) P_m(\mu) \quad (40)$$

where

$$\hat{g}_{im}(r) = \frac{1}{N_m} \int_{\mu_p}^1 g_i(r, \mu) P_m(\mu) d\mu. \quad (41)$$

Similarly, $C_{in}(\mu)$ and $C_{out}(\mu)$ in boundary conditions given by Eqs. (18) and (19) may be expanded in a generalized Fourier series to yield boundary conditions for ODE given in Eq. (39). Interface conditions for $T_{ss,i}(r, \mu)$, given in Eqs. (21) and (22), are also valid for $\hat{T}_{im}(r)$.

Solution for Eq. (39) may be written as:

$$\hat{T}_{im}(r) = A_{ss,i} r^{\beta_m} + B_{ss,i} r^{-\beta_m-1} + f_p(r) \quad (42)$$

where $f_p(r)$ is particular integral that can be obtained by application of method of variation of parameters or method of undetermined coefficients. Constants $A_{ss,i}$ and $B_{ss,i}$ may be evaluated using boundary and interface conditions for $\hat{T}_{im}(r)$.

6. Illustrative example

A three-layer hemispherical region ($r_0 \leq r \leq r_3$, $0 \leq \theta \leq \pi/2$; see Fig. 3) is initially at a uniform zero temperature. For time $t > 0$, the base of the hemisphere at $\theta = \pi/2$ as well as inner radial surface at $r = r_0$ is maintained at a uniform and constant (zero) temperature, while heat is convected into ambient, also at zero temperature, at the outer radial surface at $r = r_3$. These boundary conditions lead to $A_{in} = 0$, $B_{in} = 1$, $A_{out} = k_3$, $B_{out} = h_{out}$, $C_{in} = 0$

Table 1
Radial eigenvalues λ_{imp} for the three-layer illustrative problem.

p	$m = 1$	$m = 3$	$m = 5$	$m = 7$	$m = 9$	$m = 11$	$m = 13$	$m = 15$	$m = 17$	$m = 19$
1	1.29277	2.34254	3.46003	4.57605	5.6782	6.76164	7.8274	8.87976	9.92315	10.9608
2	2.10969	2.99396	4.12218	5.29595	6.44482	7.54839	8.63877	9.73342	10.8299	11.9244
3	3.14826	3.73857	4.5793	5.53735	6.56868	7.66152	8.77274	9.87789	10.9744	12.0634
4	4.36281	4.88525	5.7218	6.74811	7.85175	8.97043	10.0924	11.2195	12.3513	13.4847
5	5.41541	5.81587	6.48474	7.36378	8.40086	9.53865	10.7168	11.8973	13.0654	14.2112
6	6.53354	6.88794	7.48193	8.25761	9.15505	10.1229	11.1270	12.1508	13.1895	14.2495
7	7.79238	8.09242	8.61171	9.32296	10.1972	11.2013	12.2902	13.4098	14.5239	15.6318
8	8.95792	9.20332	9.63097	10.2211	10.9523	11.8052	12.7653	13.8235	14.9595	16.1341
9	10.0519	10.2867	10.6986	11.2713	11.9841	12.8135	13.7329	14.7139	15.7297	16.7616
10	11.2240	11.4327	11.8008	12.3173	12.9693	13.7440	14.6306	15.6181	16.6902	17.8198

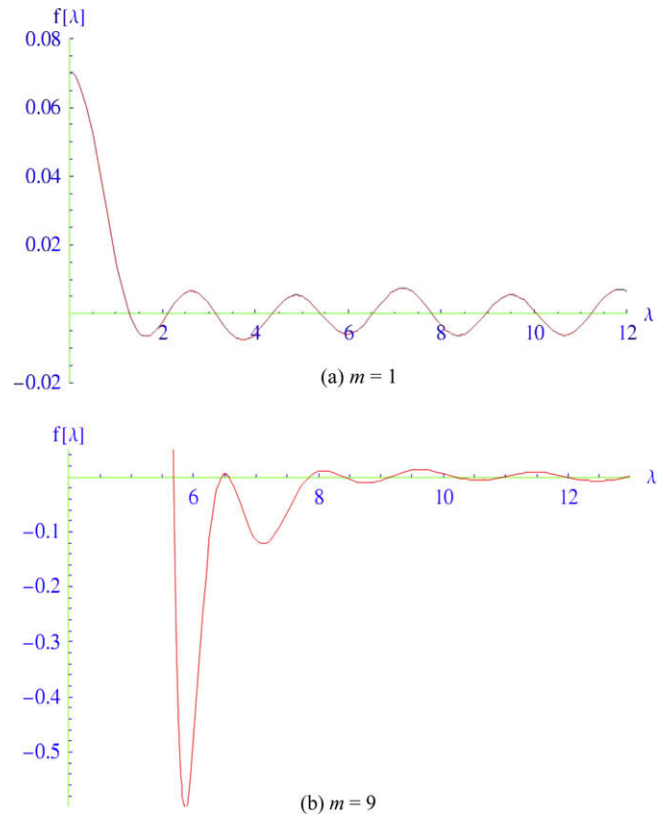


Fig. 4. Plot of eigencondition $f[\lambda]$ against λ for $m=1$ and 9. Roots of the transcendental eigencondition are obtained by using Mathematica [27] and are graphically verified by plotting $f[\lambda]$.

and $C_{out} = 0$. In addition, uniformly distributed heat source of magnitude S is turned on at $t = 0$ in the second (middle) layer.

Parameter values used for this problem are,

$$k_2/k_1 = 2, k_3/k_1 = 4; \alpha_2/\alpha_1 = 4, \alpha_3/\alpha_1 = 9; r_1/r_0 = 2, r_2/r_0 = 4, r_3/r_0 = 6, \text{Biot number } Bi_{out} \equiv h_{out} r_0/k_1 = 1.$$

It should be noted that, in the results that follow, r , t , and $T(r, \theta, t)$ are in the units of r_0 , r_0^2/α_1 and Sr_0^2/k_1 , respectively.

Steady-state solution for this problem is,

$$T_{ss,i}(r, \mu) = \sum_{m=1,3,5,\dots}^{\infty} \hat{T}_{im}(r) P_m(\mu), \quad i = 1, 2, 3 \quad (43)$$

where

$$\hat{T}_{im}(r) = A_{ss,i} r^m + B_{ss,i} r^{-m-1}, \quad i = 1, 3 \quad (44)$$

$$\hat{T}_{2m}(r) = A_{ss,1} r^m + B_{ss,1} r^{-m-1} + c_s r^2, \quad i = 2 \quad (45)$$

$$\text{and } c_s = \frac{-(2m+1)S}{k_2(6-m(m+1))} \int_0^1 P_m(\mu) d\mu.$$

The constants $A_{ss,i}$ and $B_{ss,i}$ ($i = 1, 2$ and 3) in Eqs. (44) and (45) can be evaluated by applying the steady-state interface and boundary conditions, which result in the following matrix equation:

window size has to be kept very small in order not to miss any eigenvalue. Moreover, resulting eigenvalues are verified graphically to make sure that all eigenvalues within the interval were indeed cap-

$$\begin{bmatrix} A_{ss,1} \\ B_{ss,1} \\ A_{ss,2} \\ B_{ss,2} \\ A_{ss,3} \\ B_{ss,3} \end{bmatrix} = \begin{bmatrix} (A_{in}m + B_{in}r_0)r_0^{m-1} & \{-A_{in}(m+1) + B_{in}r_0\}r_0^{-m-2} & 0 & 0 & 0 & 0 & 0 \\ r_1^m & r_1^{-m-1} & -r_1^m & -r_1^{-m-1} & 0 & 0 & 0 \\ 0 & 0 & r_2^m & r_2^{-m-1} & -r_2^m & -r_2^{-m-1} & 0 \\ k_1mr_1^{m-1} & -k_1(m+1)r_1^{-m-2} & -k_2mr_1^{m-1} & k_2(m+1)r_1^{-m-2} & 0 & 0 & 0 \\ 0 & 0 & k_2mr_2^{m-1} & -k_2(m+1)r_2^{-m-2} & -k_3mr_2^{m-1} & k_3(m+1)r_2^{-m-2} & 0 \\ 0 & 0 & 0 & 0 & (A_{out}m + B_{out}r_3)r_3^{m-1} & \{-A_{out}(m+1) + B_{out}r_3\}r_3^{-m-2} & 0 \end{bmatrix}^{-1} \begin{bmatrix} 0 \\ c_s r_1^2 \\ -c_s r_2^2 \\ 2k_2 c_s r_1 \\ -2k_2 c_s r_2 \\ 0 \end{bmatrix} \quad (46)$$

There exist infinite number of radial eigenvalues (indexed by p) for the first layer, λ_{1mp} , for each m . These eigenvalues (λ_{1mp}) are calculated by solving the transcendental eigencondition, corresponding to Eq. (35) i.e. $f[\lambda] = 0$, with the help of Mathematica [27], a commercial mathematical package. Resulting eigenvalues for various values of m and p are shown in Table 1. Roots are searched in a user-defined window of size $\Delta\lambda$ using in-built functions. Successive eigenvalues are obtained by marching forward in steps of $\Delta\lambda$ starting from zero. Since the roots are not distributed uniformly, the

tured. In Fig. 4, the variation of eigencondition $f[\lambda]$ with λ is shown graphically for $m = 1$ and $m = 9$ in order to demonstrate the viability of root-finding mechanism employed. The abovementioned scheme is not very efficient because a very small window size is required. Several methods have been reported in literature to efficiently compute eigenvalues for 2D Cartesian multilayer problems [12,14]. Further research is necessary to develop an efficient and automated scheme for the current problem, which also guarantees that all eigenvalues are captured.

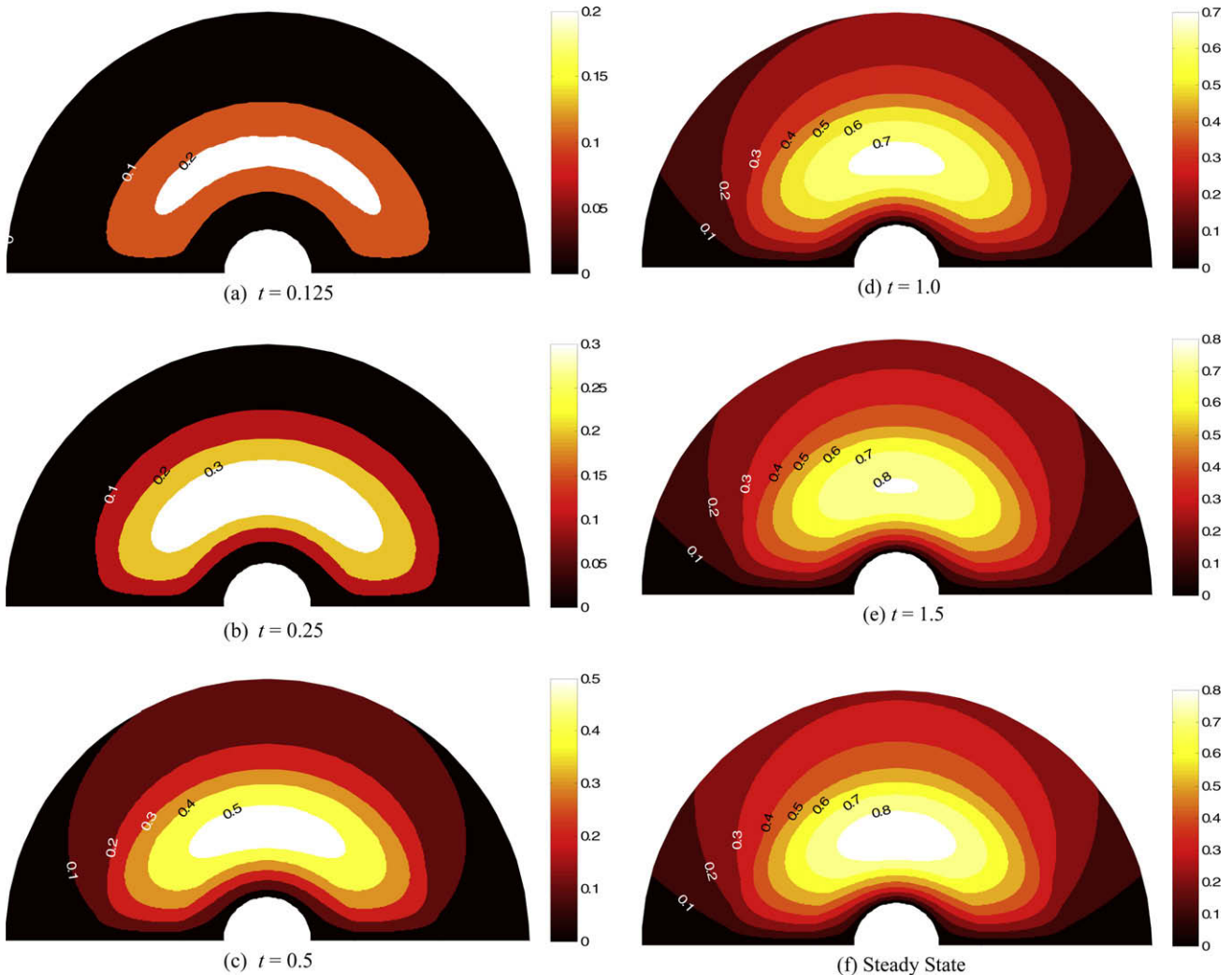


Fig. 5. Isotherms in the three-layer hemisphere at different times. Two-dimensional contours are plotted for (any) cross-sectional plane which cuts through the axis of the hemisphere.

7. Results

The transient part of the series solution for the illustrative problem described in Section 6 is truncated at $p = P$ and $m = M$, leading to,

$$\bar{T}_i(r, \mu, t) = \sum_{m=1,3,5\dots}^{OddM} \sum_{p=1}^P D_{mp} e^{-\alpha_1 \lambda_{imp}^2 t} [a_{imp} R_j(\lambda_{imp} r) + b_{imp} R_Y(\lambda_{imp} r)] P_m(\mu) + \varepsilon_i(r, \mu, t, M, P) \tag{47}$$

where $\varepsilon_i(r, \mu, t, M, P)$ is the truncation error.

Since λ_{1mp} increases with increasing m and p , it is obvious that for a given M and P , maximum truncation error occurs at $t = 0$. Moreover, since $\bar{T}_i(r, \mu, t = 0) = -T_{ss,i}(r, \mu)$, therefore,

$$\varepsilon_i(r, \mu, t = 0, M, P) = T_{ss,i}(r, \mu) + \sum_{m=1,3,5\dots}^{OddM} \sum_{p=1}^P D_{mp} [a_{imp} R_j(\lambda_{imp} r) + b_{imp} R_Y(\lambda_{imp} r)] P_m(\mu) \tag{48}$$

Numerical results show that error progressively decreases with increasing values of M and P . Moreover, for $M = 19$ and $P = 10$, trun-

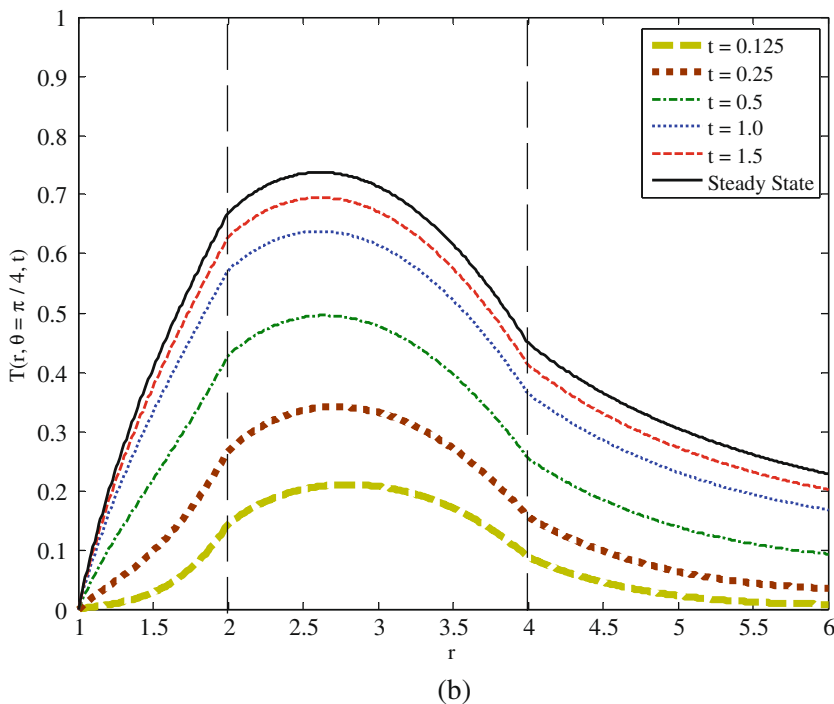
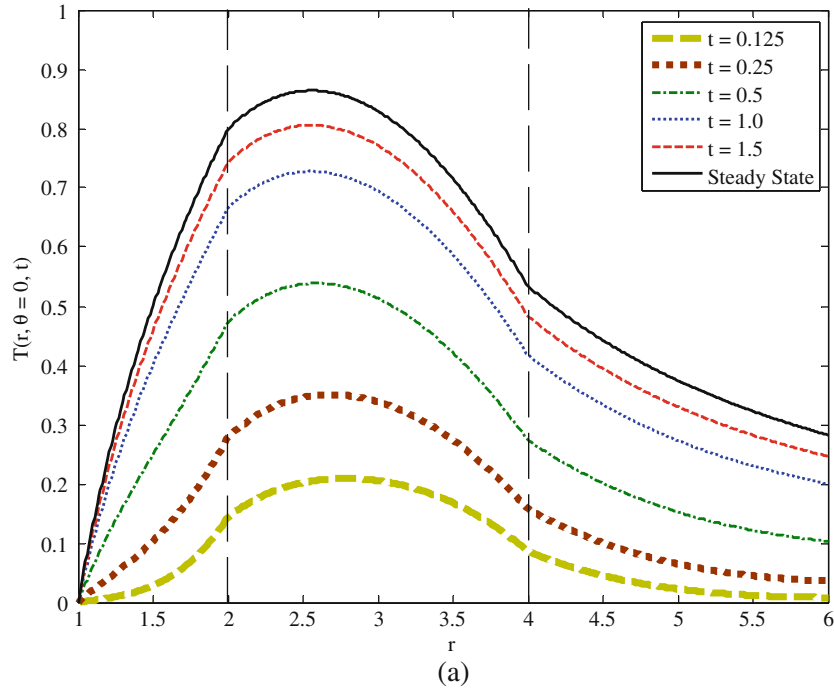


Fig. 6. Transient temperature distribution in the radial direction along $\theta = 0$ and $\theta = \pi/4$.

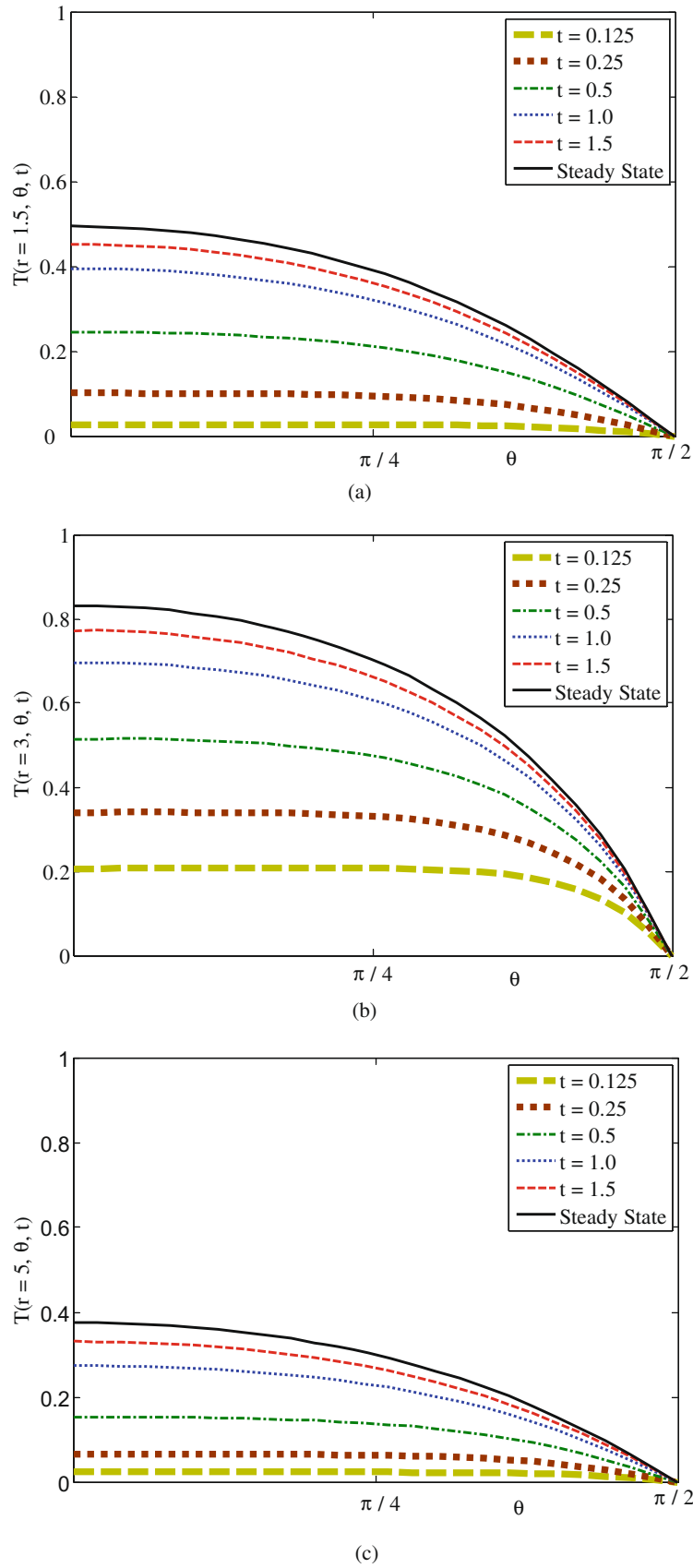


Fig. 7. Transient temperature distributions in polar direction at the mid-sections of the three layers in the hemisphere: (a) $r = 1.5$, (b) $r = 3.0$, and (c) $r = 5.0$.

cation error becomes reasonably small (order of 10^{-3}) and therefore, series is truncated for these values of M and P .

Isotherms in the three-layer hemispherical region are shown for different values of t in Fig. 5. Additionally, temperature variations along radial and polar directions are shown in Figs. 6 and 7, respectively. The steady-state solution is also shown for all the cases. It may be noted that the unsteady isotherms (in Fig. 5) and temperature variation in the radial direction (in Fig. 6) show jump in derivative at the layer interfaces due to step change in material properties.

8. Conclusions

In this paper, exact analytical solution to the 2D, transient heat conduction problem in spherical coordinate (r - θ) with multiple layers in the radial direction is presented. The solution is valid for a variety of spherical and *part*-spherical, azimuthally symmetric, multilayer geometries, such as spherical cone and wedge, hemisphere and full sphere. In fact, the solution gets significantly simpler in more practically relevant spherical geometry – hemisphere and full sphere – because of integer eigenvalues in the θ direction. Proposed solution is valid for any combination of homogenous boundary condition of the *first* or *second* kind at the θ -boundaries. However, inhomogeneous boundary condition of the *first*, *second* or the *third* kind can be applied in the radial direction. Proposed solution is also applicable to a geometry with zero inner radius. Numerical evaluation of the double series solution shows that a reasonable number of terms are sufficient to obtain results with acceptable errors for engineering applications.

It is noted that the solution of multilayer, two-dimensional heat conduction problem in spherical coordinates is not analogous to the corresponding problem in multi-dimensional Cartesian coordinates (or 2D cylindrical r - z coordinates). In the spherical coordinates, dependence of the radial eigenvalues on those in the polar direction is not explicit. Absence of explicit dependence leads to a complete solution which does not have imaginary radial eigenvalues.

The solution of the multilayer heat conduction problem in the spherical coordinates can not be trivially deduced from the corresponding problems in the cylindrical or polar coordinates. Reason being that except for the special cases of $\Psi = \pi/2$ and $\Psi = \pi$, an eigenvalue problem has to be solved in the angular direction to obtain eigenvalues β_m . This leads to differences in computations of radial eigenvalues due to their dependence on the angular eigenvalues β_m .

References

- [1] C.W. Tittle, Boundary value problems in composite media: quasi-orthogonal functions, *J. Appl. Phys.* 36 (4) (1965) 1486–1488.
- [2] P.E. Ulavina, V.M. Kascreev, Solution of the non-homogeneous heat conduction equation for multilayered bodies, *Int. Chem. Eng.* 1V (1965) 112–115.
- [3] G.P. Mulholland, M.H. Cobble, Diffusion through composite media, *Int. J. Heat Mass Transfer* 15 (1972) 147–160.
- [4] S.C. Huang, Y.P. Chang, Heat conduction in unsteady, periodic and steady states in laminated composites, *J. Heat Transfer (Trans. ASME)* 102 (1980) 742–748.
- [5] M.D. Mikhailov, M.N. Ozisik, N.L. Vulchanov, Diffusion in composite layers with automatic solution of the eigenvalue problem, *Int. J. Heat Mass Transfer* 26 (8) (1983) 1131–1141.
- [6] H. Salt, Transient heat conduction in a two-dimensional composite slab. I. Theoretical development of temperatures modes, *Int. J. Heat Mass Transfer* 26 (11) (1983) 1611–1616.
- [7] H. Salt, Transient heat conduction in a two-dimensional composite slab. II. Physical Interpretation of temperatures modes, *Int. J. Heat Mass Transfer* 26 (11) (1983) 1617–1623.
- [8] M.D. Mikhailov, M.N. Ozisik, Transient conduction in a three-dimensional composite slab, *Int. J. Heat Mass Transfer* 29 (2) (1986) 340–342.
- [9] R. Siegel, Transient thermal analysis of parallel translucent layers by using Green's functions, *J. Thermophys. Heat Transfer (AIAA)* 13 (1) (1999) 10–17.
- [10] F. de Monte, Transient heat conduction in one-dimensional composite slab. A 'natural' analytic approach, *Int. J. Heat Mass Transfer* 43 (19) (2000) 3607–3619.
- [11] F. de Monte, An analytic approach to the unsteady heat conduction processes in one-dimensional composite media, *Int. J. Heat Mass Transfer* 45 (6) (2002) 1333–1343.
- [12] A. Haji-Sheikh, J.V. Beck, Temperature solution in multi-dimensional multilayer bodies, *Int. J. Heat Mass Transfer* 45 (9) (2002) 1865–1877.
- [13] F. de Monte, Unsteady heat conduction in two-dimensional two slab-shaped regions. Exact closed-form solution and results, *Int. J. Heat Mass Transfer* 46 (8) (2003) 1455–1469.
- [14] F. de Monte, Transverse eigenproblem of steady-state heat conduction for multi-dimensional two-layered slabs with automatic computation of eigenvalues, *Int. J. Heat Mass Transfer* 47 (2004) 191–201.
- [15] Y. Sun, I.S. Wichman, On transient heat conduction in a one dimensional composite slab, *Int. J. Heat Mass Transfer* 47 (2004) 1555–1559.
- [16] X. Lu, P. Tervola, M. Viljanen, A new analytical method to solve heat equation for multi-dimensional composite slab, *J. Phys. A: Math. Gen.* (38) (2005) 2873–2890.
- [17] R. Cai, C. Gou, H. Li, Algebraically explicit analytical solutions of unsteady 3D nonlinear non-Fourier (hyperbolic) heat conduction, *Int. J. Therm. Sci.* 45 (2006) 893–896.
- [18] F. de Monte, Multi-layer transient heat conduction using transition time scales, *Int. J. Therm. Sci.* 45 (2006) 882–892.
- [19] X. Lu, P. Tervola, M. Viljanen, Transient analytical solution to heat conduction in composite circular cylinder, *Int. J. Heat Mass Transfer* 49 (2006) 341–348.
- [20] X. Lu, P. Tervola, M. Viljanen, Transient analytical solution to heat conduction in multi-dimensional composite cylinder slab, *Int. J. Heat Mass Transfer* 49 (2006) 1107–1114.
- [21] S. Singh, P.K. Jain, Rizwan-uddin, Analytical solution to transient heat conduction in polar coordinates with multiple layers in radial direction, *Int. J. Therm. Sci.* 47 (2008) 261–273.
- [22] P.K. Jain, S. Singh, Rizwan-uddin, Transient analytical solution to asymmetric heat conduction in a multilayer annulus, *J. Heat Transfer* 131 (2009) 011304.
- [23] S. Singh, P.K. Jain, Rizwan-uddin, Finite integral transform technique to solve asymmetric heat conduction in a multilayer annulus with time dependent boundary conditions, *Nucl. Eng. Des.*, submitted for publication.
- [24] X. Lu, M. Viljanen, An analytical method to solve heat conduction in layered spheres with time-dependent boundary conditions, *Phys. Lett. A* 351 (2006) 274–282.
- [25] L.G. Astafyeva, N.V. Voshchinnikov, L.B.F.M. Waters, Heating of three-layer solid aerosol particles by laser radiation, *Appl. Opt.* 41 (2002) 3700–3705.
- [26] M.N. Ozisik, *Heat Conduction*, Wiley, New York, 1993.
- [27] Wolfram Research, Inc., *Mathematica*, Version 5.2, Champaign, IL, 2005.